Anisotropic Stokes Drag and Dynamic Lift on Cylindrical Colloids in a Nematic Liquid Crystal

Joel B. Rovner, Clayton P. Lapointe, Daniel H. Reich, and Robert L. Leheny

Department of Physics and Astronomy, Johns Hopkins University, Baltimore, Maryland 21218, USA

(Received 17 September 2010; published 22 November 2010)

We have measured the Stokes drag on magnetic nanowires suspended in the nematic liquid crystal 4-cyano-4'-pentylbiphenyl (5CB). The effective drag viscosity for wires moving perpendicular to the nematic director differs from that for motion parallel to the director by factors of 0.88 to 2.4, depending on the orientation of the wires and their surface anchoring. When the force on the wires is applied at an oblique angle to the director, the wires move at an angle to the force, demonstrating the existence of a lift force on particles moving in a nematic. This dynamic lift is significantly larger for wires with homeotropic anchoring than with longitudinal anchoring in the experiments, suggesting the lift force as a mechanism for sorting particles according to their surface properties.

DOI: 10.1103/PhysRevLett.105.228301 PACS numbers: 82.70.Dd, 47.57.Lj, 61.30.−v, 83.85.Jn

When colloids are suspended in a liquid crystal, the anisotropic viscoelastic properties of the medium introduce a host of novel phenomena. For example, the boundary conditions created by the anchoring of the liquid-crystal molecules at the particle surfaces introduce distortions in the nematic order, with corresponding costs in the free energy of the liquid crystal. Since the energy cost of such distortions generally depends on the position of a particle relative to its neighbors or to other bounding surfaces, the fluid can mediate interactions [1–5] that lead to striking and unexpected results, such as the levitation of particles in opposition to gravity [6–8] and the formation of stable colloidal crystals [9–11]. This makes colloids in liquid crystals valuable for exploring nematic elasticity and interfacial phenomena, particularly as they relate to topological defects, and has motivated interest in employing these anisotropic forces as a mechanism for colloidal manipulation [12] and assembly.

While particle interactions in liquid crystals have been a highly active topic of study, relatively little experimental work [13–15] has focused on the unique hydrodynamic behavior of colloids in nematic fluids. However, the dynamic response of colloids to forces in liquid crystals is a central component of their properties. For example, in many cases colloidal assemblies in nematics are metastable [2,3,11,16]. Hence, their realization can depend on the details of the colloids' motion as they assemble. Also, nanoparticles suspended in a nematic can enhance its material properties, such as its sensitivity to applied electric fields [17]. These enhancements rely on the response of the particles to the fields, again making their motion an important consideration. The study of colloidal dynamics can further provide insight into liquid-crystal hydrodynamics, a notoriously complicated subject in which few flow configurations can be analyzed in detail. Since many applications of nematics rely on flow, their viscous behavior has broad implications, making controlled experiments with simple geometries, such as can be achieved with colloids, highly valuable. Indeed, interesting predictions have been made regarding colloidal mobility, and specifically the Stokes drag on colloids, in liquid crystals [18–23]. Among the most intriguing of these is the possibility of a dynamic ''nematic lift'' force that redirects the colloid away from the direction of an applied force when the force is at an oblique angle to the nematic director [18,19]. Here, we report experiments on the Stokes drag on cylindrical colloids in a nematic that elucidate the anisotropic nature of the drag and demonstrate the existence of such a dynamic lift. The degree of anisotropy and the magnitude of the lift are sensitive to the local distorted director field near the cylinders, demonstrating the importance of colloids' surface properties on their hydrodynamic behavior.

The experiments were performed using ferromagnetic Ni nanowires in the nematic 4-cyano-4'-pentylbiphenyl (5CB). The cylindrical wires, with radius $R = 185 \pm 25$ nm and lengths L ranging from 5 to 40 μm, were fabricated using electrochemical deposition [24] and suspended in 5CB in dilute concentration [7]. The wires have large permanent magnetic dipole moments along their long axis ($\mu = 3 \times 10^{-13}$ A $\cdot$ m^2 for a 10 μm wire [24]). The bare surfaces of the wires strongly anchor the nematic director parallel to the wire's long axis, a condition known as longitudinal anchoring [6,7]. To obtain wires with homeotropic anchoring, in which the director's preferred orientation is normal to the surface, the wires were functionalized with *N*-Octadecyldimethyl[3-(Trimethoxysilyl)Propyl]Ammoniumchloride (DMOAP, United Chem. Tech.) prior to their dispersion in 5CB [25]. The 5CB/nanowire solutions were loaded into liquid-crystal cells (Instec) by capillary action while in the isotropic phase of the 5CB above 35 C. The cell substrates were treated for homogenous planar anchoring, and their spacing was 20 μm. After filling, the cells were cooled into 5CB's nematic phase slowly. All measurements were performed at room temperature.

Measurements of Stokes drag on the wires followed procedures described previously [26]. Briefly, wire motion

within the nematic was monitored via video microscopy using an inverted optical microscope (Nikon TE2000) with an extra-long-working-distance 40× objective and 1.5× zoom. A custom-designed "magnetic tweezer" stage was used to apply torques and forces to the wires through magnetic fields and field gradients. Wires were imaged with a CMOS-based camera (Photron FASTCAM 512) at a frame rate of 60 fps. Image analysis to determine the positions of wires as a function of time was conducted in the software package IGORPRO (WaveMetrics).

Drag measurements were performed on suspended wires translating both parallel and perpendicular to the wire's long axis. In each case, wires were driven with a constant magnetic force by application of a magnetic-field gradient. In general, this force can be expressed as $\mathbf{F_B} = \nabla(\boldsymbol{\mu} \cdot \mathbf{B})$ where $\boldsymbol{\mu}$ is the wire's magnetic dipole moment and $\mathbf{B}$ is the applied field. In all the measurements, the field strength at the wire position was 5 mT, which was large enough that the magnetic torque on the wires overwhelmed the elastic torque on the wires from the nematic [6], so that $\boldsymbol{\mu}$, and hence wires' long axis, aligned closely with $\mathbf{B}$. To translate wires parallel to their long axis, the field gradient was made parallel to $\mathbf{B}$, while to drive them perpendicular to their axis, the gradient in the field magnitude, and hence $\mathbf{F_B}$, was configured normal to $\mathbf{B}$ [26]. Prior to any measurements, the wires were rotated at 1 Hz by a rotating magnetic field causing them to levitate to the midplane of the cells [6], so that the drag was characterized with the wires isolated from the bounding substrates.

For a high-aspect-ratio cylindrical wire translating in an isotropic fluid, the Stokes drag force is

$$\mathbf{F_d} = -\zeta_{\parallel,\perp}\eta\mathbf{v}, \tag{1}$$

where η is the viscosity, $\mathbf{v}$ is the velocity, and $\zeta_{\parallel,\perp}$ is the geometric coefficient that depends on whether the cylinder is moving parallel to its axis, $\zeta_{\parallel} \cong 2\pi L/[\ln(L/2R) - 0.20]$, or perpendicular to it, $\zeta_{\perp} \cong 4\pi L/[\ln(L/2R) + 0.84]$ [27]. Because of the nematic's anisotropy, the nature of the drag becomes more complicated. However, if the applied force is small and is along a high-symmetry direction, either parallel or perpendicular to the far-field director $\mathbf{n}$, Eq. (1) could still be valid, albeit with a direction-dependent drag viscosity. Hence, a first question to consider is the difference in the effective drag viscosities along these high-symmetry directions. We have evaluated these viscosities for wires moving both parallel or perpendicular to their long axis, leading to four measurement configurations shown in Fig. 1. Because the wire motion is at low Reynolds number, the magnetic force and drag force balance, $\mathbf{F_B} - \mathbf{F_d} = 0$. In each case in Fig. 1, the drag viscosity should depend both on whether the velocity is parallel or perpendicular to $\mathbf{n}$, as denoted by the superscript on η, and on the orientation of the wire with respect to $\mathbf{n}$ since different orientations lead to different distorted director fields around the wire [6,7,28]. We denote

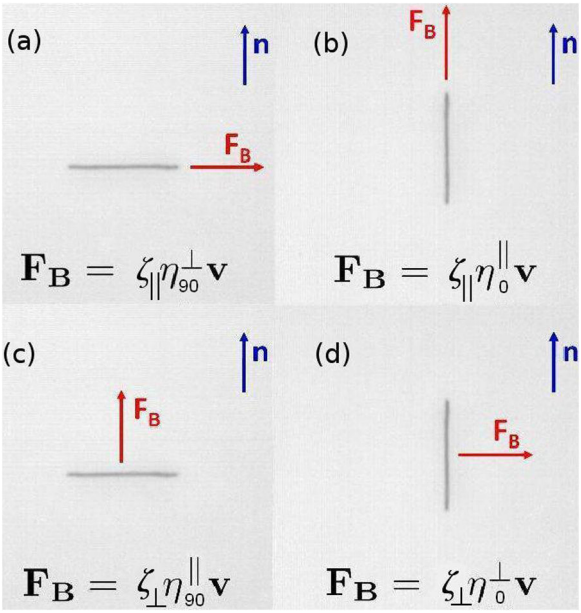

FIG. 1 (color online). Annotated micrographs of a nanowire in a nematic specifying the four configurations in which the drag is determined. The wire translates in response to an applied magnetic force $\mathbf{F_B}$ along the high-symmetry directions parallel or perpendicular to the far-field director $\mathbf{n}$.

this degree of freedom by the subscript on η, which gives the angle θ between the wire axis and $\mathbf{n}$.

Figure 2 displays results of measurements on a wire with longitudinal anchoring moving parallel to its axis both for $\mathbf{v} \parallel \mathbf{n}$ [as in Fig. 1(b)] and for $\mathbf{v} \perp \mathbf{n}$ [as in Fig. 1(a)]. In each case, the magnetic-field gradient was varied between 0.25 and 0.50 T/m, and the measurements were repeated with the field gradient reversed so that the wire motion was reversed. Similar measurements were performed on wires moving perpendicular to their axis [as in Figs. 1(c) and 1(d)] and on wires with homeotropic anchoring. In all cases, the wire velocity was proportional to the applied force, indicating the motion was in the linear regime of low Ericksen number where the nematic order is unaffected by the flow [29] and enabling us to identify effective drag viscosities through Eq. (1).

The drag viscosities determined from these measurements ranged from 25 mPa · s to 110 mPa · s. These fall in the same range as the Miesowicz coefficients of 5CB at room temperature, which are $\eta_1 = 133$ mPa · s, $\eta_2 = 22$ mPa · s, and $\eta_3 = 52$ mPa · s [30]. (The Miesowicz coefficients are the viscosities for uniform shear with the shear velocity $\mathbf{u}$ and velocity gradient ∇u along high-symmetry directions: η_1 for $\mathbf{n} \parallel \nabla\mathbf{u}$, η_2 for $\mathbf{n} \parallel \mathbf{u}$, and η_3 for $\mathbf{n} \perp \mathbf{u}$ and $\mathbf{n} \perp \nabla\mathbf{u}$.) However, rather than focus on the viscosities themselves, we examine their ratios, which illustrate directly the anisotropy in the Stokes drag. Viscosity ratios for different pairs of measurement configurations are listed in Table I for both longitudinal and homeotropic anchoring. In each anchoring condition, the

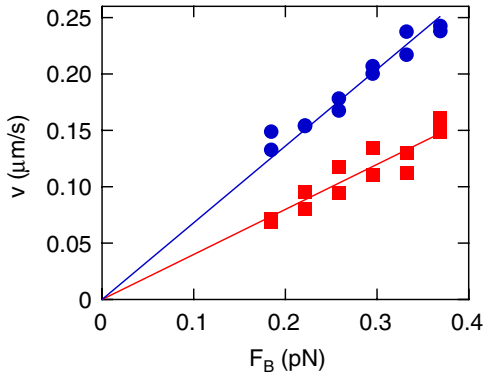

FIG. 2 (color online). Velocity of a nanowire of length 25 μm with longitudinal anchoring as a function of applied magnetic force along the wire axis for the force parallel to the far-field director (blue circles) and perpendicular to the director (red squares). The lines are the results of fits to Eq. (1) from which the effective drag viscosity in each case is obtained.

full set of ratios was determined for at least four wires, and the quoted values are the averages. Of these ratios, perhaps the most interesting are $\eta_0^{\perp}/\eta_0^{\parallel}$ and $\eta_{90}^{\perp}/\eta_{90}^{\parallel}$ since for these the numerator and denominator correspond to the same wire orientation with respect to $\mathbf{n}$ and hence to the same distorted director field around the wire. For example, for $\eta_0^{\perp}/\eta_0^{\parallel}$ the wire is parallel to the director, and hence for longitudinal anchoring the director field is undistorted [6,7]. Thus, when the wire moves parallel to $\mathbf{n}$, leading to $\eta_0^{\parallel}$, the shear flow should be exclusively parallel to the director, which corresponds to the geometry for Miesowicz coefficient η_2. When the wire with longitudinal anchoring at this orientation moves moves perpendicular to the director, leading to the $\eta_0^{\perp}$, the flow should predominately have a shear velocity and velocity gradient perpendicular to $\mathbf{n}$, the geometry for η_3. Thus, one should expect $\eta_0^{\perp}/\eta_0^{\parallel} \approx \eta_3/\eta_2 = 2.4$, in close agreement with the measured value. When the wire with longitudinal anchoring is rotated by 90° with respect to $\mathbf{n}$ as in $\eta_{90}^{\perp}/\eta_{90}^{\parallel}$, the director near the wire is obligated to rotate as well [6,7], changing locally

TABLE I. Ratios of the effective drag viscosities for cylindrical wires with longitudinal and homeotropic surface anchoring translating in nematic 5CB for different configurations of wire orientation and velocity direction as specified Fig. 1.

Longitudinal	
$\eta_{90}^{\perp}/\eta_0^{\parallel} = 1.75 \pm 0.03$	$\eta_0^{\perp}/\eta_{90}^{\parallel} = 1.17 \pm 0.02$
$\eta_0^{\perp}/\eta_0^{\parallel} = 2.38 \pm 0.05$	$\eta_{90}^{\perp}/\eta_{90}^{\parallel} = 0.88 \pm 0.03$
Homeotropic	
$\eta_{90}^{\perp}/\eta_0^{\parallel} = 1.54 \pm 0.04$	$\eta_0^{\perp}/\eta_{90}^{\parallel} = 1.44 \pm 0.09$
$\eta_0^{\perp}/\eta_0^{\parallel} = 2.0 \pm 0.1$	$\eta_{90}^{\perp}/\eta_{90}^{\parallel} = 1.10 \pm 0.05$

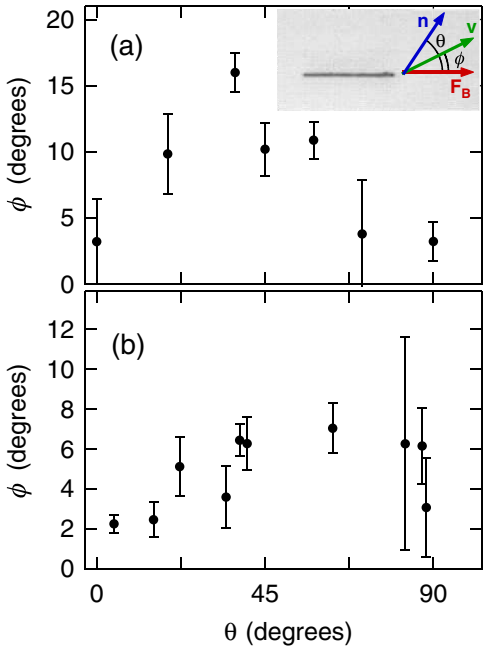

FIG. 3 (color online). Angle of deflection ϕ between the external force and resulting wire velocity, indicating dynamic lift, as a function of the angle between the force and the director θ for wires with (a) homeotropic and (b) longitudinal anchoring. The inset to (a) displays an annotated micrograph showing the experimental geometry.

the relative orientations of $\mathbf{n}(\mathbf{r})$ and $\mathbf{u}$. This distortion of the director field around the wire conspires with the flow field to alter dramatically the anisotropy in the drag so that the viscosity for motion perpendicular to the director actually becomes smaller than that parallel to it, $\eta_{90}^{\perp}/\eta_{90}^{\parallel} = 0.88 \pm 0.03$. This change in anisotropy with wire orientation thus illustrates the strong impact of the nearby distorted director field on a particle's Stokes drag. As seen in Table I, the trend for $\eta_0^{\perp}/\eta_0^{\parallel}$ and $\eta_{90}^{\perp}/\eta_{90}^{\parallel}$ for wires with homeotropic anchoring is similar but less pronounced.

As mentioned above, an interesting anticipated consequence of the anisotropy in the nematic is a dynamic lift on a particle generated by the liquid crystal when the external force is at an oblique angle to the director. Specifically, Ruhwandl and Terentjev have predicted such a lift force on both cylinders [18] and spheres [19] moving in a nematic. To test for a lift force on the nanowires, we conducted measurements illustrated schematically in the inset to Fig. 3(a). The external force $\mathbf{F_B}$ was applied at an angle θ to $\mathbf{n}$. In the presence of a lift force, the wire velocity $\mathbf{v}$ should have a component perpendicular to the force so that the velocity makes an angle ϕ with respect to $\mathbf{F_B}$. We define ϕ to be positive if the deflection of the velocity is toward $\mathbf{n}$. The measurements focused on the case in which $\mathbf{F_B}$ was parallel to the wire axis, since in this orientation we could determine the direction of the force with greatest precision. Figures 3(a) and 3(b) show the results for ϕ as a function of θ for wires with homeotropic and longitudinal

anchoring, respectively. As expected, ϕ approaches zero when the wire moves along the high-symmetry directions, $\theta = 0°$ and 90°. However, for homeotropic anchoring, a pronounced lift is observed when θ is at an oblique angle, with ϕ exceeding 15° when $\theta \approx 40°$. For nanowires with longitudinal anchoring, a lift is also observed but with significantly smaller magnitude. For example, $\phi \approx 6°$ at $\theta = 40°$ for this case.

We stress that this lift force is distinct from the hydrodynamic lift that a prolate particle like a cylinder experiences as part of the Stokes drag in an isotropic fluid when the applied force is at an oblique angle to the particle's long axis [31]. In the present experiments, the applied force is along the particle's axis, a geometry that would not cause hydrodynamic lift. Further, as the dependence of ϕ on θ shows, the velocity only deviates from this direction due to the relative orientation of $\mathbf{n}$, demonstrating that the result is a direct consequence of the nematic's anisotropy. Indeed, since the effect of hydrodynamic lift is to redirect the particle velocity toward the direction of the particle's long axis [31], its only effect in these experiments could be to counter the lift caused by the nematic.

Since such dynamic lift should be a generic consequence of a nematic's anisotropy, one can expect that its existence, demonstrated here for cylinders, is a common feature of colloid mobility in liquid crystals. An interesting possibility that the lift introduces is the ability to sort particles due to their surface anchoring [23]. The surface properties of objects such as nanoparticles and biomolecular complexes are crucial to their technological application, and recent work has emphasized how the different distortions of the nematic director around such objects can be an effective signature for distinguishing these properties [32,33]. The sensitivity of the strength of the dynamic lift to anchoring conditions demonstrated in the contrasting deflection angles in Figs. 3(a) and 3(b) further suggests the possibility that such objects can be sorted through their Stokes drag.

Funding was provided by the NSF (DMR-0706021).

[1] P. Poulin, V. Cabuil, and D. A. Weitz, Phys. Rev. Lett. **79**, 4862 (1997).
[2] M. Yada, J. Yamamoto, and H. Yokoyama, Phys. Rev. Lett. **92**, 185501 (2004).
[3] I. I. Smalyukh *et al.*, Phys. Rev. Lett. **95**, 157801 (2005).
[4] J. Kotar *et al.*, Phys. Rev. Lett. **96**, 207801 (2006).
[5] G. M. Koenig, J. J. de Pablo, and N. L. Abbott, Langmuir **25**, 13318 (2009).
[6] C. Lapointe *et al.*, Science **303**, 652 (2004).
[7] C. Lapointe *et al.*, J. Appl. Phys. **97**, 10Q304 (2005).
[8] O. P. Pishnyak *et al.*, Phys. Rev. Lett. **99**, 127802 (2007).
[9] V. G. Nazarenko, A. B. Nych, and B. I. Lev, Phys. Rev. Lett. **87**, 075504 (2001).
[10] I. Muševič *et al.*, Science **313**, 954 (2006).
[11] U. Ognysta *et al.*, Phys. Rev. Lett. **100**, 217803 (2008).
[12] C. P. Lapointe, D. H. Reich, and R. L. Leheny, Langmuir **24**, 11 175 (2008).
[13] J. C. Loudet, P. Hanusse, and P. Poulin, Science **306**, 1525 (2004).
[14] A. A. Verhoeff *et al.*, Soft Matter **4**, 1602 (2008).
[15] H. F. Gleeson, T. A. Wood, and M. Dickinson, Phil. Trans. R. Soc. A **364**, 2789 (2006).
[16] M. Ravnik *et al.*, Phys. Rev. Lett. **99**, 247801 (2007).
[17] Y. Reznikov *et al.*, Appl. Phys. Lett. **82**, 1917 (2003).
[18] R. W. Ruhwandl and E. M. Terentjev, Z. Naturforsch. Teil A **50**, 1023 (1995).
[19] R. W. Ruhwandl and E. M. Terentjev, Phys. Rev. E **54**, 5204 (1996).
[20] J. L. Billeter and R. A. Pelcovits, Phys. Rev. E **62**, 711 (2000).
[21] H. Stark and D. Ventzki, Phys. Rev. E **64**, 031711 (2001).
[22] H. Stark and D. Ventzki, Europhys. Lett. **57**, 60 (2002).
[23] T. Araki and H. Tanaka, J. Phys. Condens. Matter **18**, L193 (2006).
[24] A. Hultgren *et al.*, J. Appl. Phys. **93**, 7554 (2003).
[25] C. M. Noel *et al.*, Colloids Surf. A **295**, 246 (2007).
[26] M. H. Lee *et al.*, Langmuir **25**, 7976 (2009).
[27] M. M. Tirado and J. G. de la Torre, J. Chem. Phys. **71**, 2581 (1979).
[28] Wires with longitudinal anchoring prefer to orient parallel to $\mathbf{n}$ [6,7], while homeotropic wires prefer to be perpendicular to $\mathbf{n}$. The distortions introduced by rotating the wires to the other orientations (perpendicular to $\mathbf{n}$ for longitudinal, parallel for homeotropic) break the symmetry, which some measurements indicated made the drag more complicated than suggested by Eq. (1). However, these small effects were typically outweighed by other uncertainties, and we neglect them here.
[29] Within a one-elastic-constant approximation, the Ericksen number $\mathrm{Er} = \eta v L/K$, where $K \approx 10^{-11}$ N is the average Frank elastic constant. For the observed wire velocities, $v \lesssim 0.25\ \mu$m/s, $\mathrm{Er} \approx 10^{-2}$.
[30] A. G. Chmielewski, Mol. Cryst. Liq. Cryst. **132**, 339 (1986).
[31] J. Happel and H. Brenner, *Low Reynolds Number Hydrodynamics* (Prentice Hall, Englewood Cliffs, NJ, 1965).
[32] S. V. Shiyanovskii *et al.*, Phys. Rev. E **71**, 020702 (2005).
[33] G. M. Koenig *et al.*, Nano Lett. **9**, 2794 (2009).